JOINT EUROPEAN TORUS

JET–P(91)58

J. Jacquinot, M. Bures
and JET Team

JET Results with both Fast and Lower Hybrid Waves Consequences for Future Devices

X JET Results with both Fast and Lower Hybrid Waves Consequences for Future Devices

J. Jacquinot, M. Bures
and JET Team*

JET-Joint Undertaking, Culham Science Centre, OX14 3DB, Abingdon, UK

** See Appendix 1*

Preprint of Paper to be submitted for publication in
a special issue of Physics of Fluids

JET RESULTS WITH BOTH FAST AND LOWER HYBRID WAVES CONSEQUENCES FOR FUTURE DEVICES

J Jacquinot, M Bures and the JET Team

JET Joint Undertaking, Abingdon, Oxon OX14 3EA, UK

Abstract

Heating and Current Drive studies were performed during the JET 1990/91 operation using 2 large systems capable of generating either fast waves in the Ion Cyclotron Range of Frequencies (ICRF) or slow waves at a frequency above the Lower Hybrid resonance (LH). The maximum wave power coupled to the torus reached 22 MW for ICRH and 2.4 MW for LH. The results obtained in plasma heating experiments qualify ICRH as a prime candidate for heating reactor grade plasmas. A centrally localized deposition profile in the cyclotron damping regime was demonstrated in a wide range of plasma density resulting in: (i) record value $n_d \tau_{io} T_{io} \simeq 7.8\ 10^{20}$ m^{-3} s keV in "thermal" conditions $T_i = T_e \simeq 11$ keV at high central densities generated by pellet injection, (ii) large normalised confinement $2.5 \leq \tau_E/\tau_{Goldston} \leq 4$. The large values of $\tau_E/\tau_{Goldston}$ are reached in H-mode discharges ($I \leq 1.5$ MA) with large bootstrap current fraction $I_{BS}/I \leq 0.7 \pm 0.2$, (iii) the highest to date D-^{3}He fusion power (140 kW) generated with 10 - 14 MW of ICRH in the L-mode regime at the ^{3}He cyclotron frequency. All specific impurity generations have been reduced to negligible levels by proper antenna design and the generic difficulty of wave-plasma coupling has been greatly reduced using feedback loops controlling in real time the antenna circuits and the plasma position.

Current Drive efficiencies $\gamma = I_{CD} < n_e > R/P \simeq 0.4\ 10^{20}$ m^{-2} A/W have been reached in 1.5 MA L-mode plasma with zero loop voltage by combining LHCD and ICRH. Fast electrons are driven by LHCD alone to tail temperatures of up to 70 keV. The fast electron density is peaked in the plasma center at lower densities ($n_{eo} \leq 2.6\ 10^{19}$ m^{-3}) and high field ($B_\phi \sim 3.1$ T). In these conditions, the fast electrons are further accelerated (even at zero loop voltage) to tail temperatures above 150 keV by heating the plasma with ICRF in monopole

phasing. Direct electron damping of the fast wave on the fast electron created by LH appears to be the driving mechanism of this synergism which produces fast wave current drive even without phasing the ICRH antennae. Finally, we report the first results obtained in the minority current drive regime. The sawtooth instability is considerably modified when the resonance is located near the q = 1 resonance. The effect is reversed from stabilisation to destabilisation when the phase of the ICRH antennae is reversed from +90° to -90°.

I.INTRODUCTION

The fusion research programs have obtained considerable success in the development of auxiliary systems suitable for heating a reactor grade plasma confined in magnetic toroidal devices[1]. The research in this field now concentrates on extending the use of these methods to other applications such as current drive, profile control and burn control suitable for a burning plasma in quasi-steady state. Whilst providing these new services, the auxiliary system should maintain its ability for heating. The plasma parameters of a burning fusion plasma are not yet precisely known as there are conflicting requirements: the plasma density should be high so that the divertor power loading can remain acceptable. On the contrary, current drive and burn control aspects would favour a lower density in order to increase the current drive efficiency and to reduce the thermal instability in the ignition regime. Therefore there is a considerable incentive to develop heating and current drive systems with the flexibility of working in a wide range of plasma conditions and with the capability of serving different functions.

The Joint European Torus (JET) has constructed 2 large systems in the radio and microwave frequency ranges and the subject of this article is to review the results obtained during the 2 JET experimental campaigns conducted in 1990 and 1991 and to draw the consequences for future devices. The 1990 results were presented recently[2] and will be briefly mentioned here when necessary for the coherence of the discussion. The new results obtained in 1991 concern: the minority fast wave current drive regime, zero loop voltage operation with LHCD, high bootstrap current operation combined with high τ_E/τ_{EG} using ICRH (τ_{EG} refers to the Goldston Aachen scaling)[3] and synergistic effects between LHCD and ICRH. The

present article will concentrate on these results leading to a discussion on the remaining uncertainties in the use of these 2 RF systems for Next Step devices.

II.THE PHYSICS GUIDELINES OF ICRH AND LHCD

The Lower Hybrid system launches slow waves at 3.7 GHz. The wave electric field is nearly parallel to the magnetic field. It is generated at the plasma boundary by a waveguide array. The frequency is above the threshold value for any significant cyclotron damping on thermal ions and the wave is damped by Electron Landau (EL) damping giving parallel energy to plasma electrons moving at the wave phase velocity ($\omega = k_{//} v_{//}$ or $v_{//} = c/n_{//}$). In JET $n_{//} \simeq$ 1.8 meaning that the wave is resonant with 100 keV electrons. A high energy tail is formed in plasmas with low electron collisionality. The accessibility and damping conditions prevent the wave from penetrating further than a critical density. In JET the critical density is about 2.5 10^{19} m^{-3} at 3.4 T. The wave penetration is improved at higher field, higher frequency and when the density profile is peaked.

The ICRH system launches fast waves generating an electric field nearly perpendicular to the magnetic field. The wave propagates along the density gradient and focuses near the magnetic axis. Cyclotron absorption by a minority ion species (^{3}He or H in this work) is a powerful damping mechanism providing close to single pass damping in the H minority case. Perpendicular energy is transferred to the minority ions. The power deposition is centrally peaked when the ion cyclotron (IC) resonance is adjusted to be near the magnetic axis. There is no limit to the plasma density that the wave can penetrate. Another weaker damping mechanism, the Transit Time Magnetic Pumping has recently been demonstrated in JET[4]. It can only be significant in large plasmas with high electron energy content or, as in this work, when fast electrons are already present. When both IC and TTMP damping are present, the former invariably dominates. To obtain a significant electron heating by the TTMP damping on JET the cyclotron layer has to be shifted from the magnetic axis[4] so as to degrade the efficiency of the IC damping. In the experiments on synergism between Lower Hybrid waves and the Fast waves discussed in Section B, the direct electron damping is possibly enhanced by the presence of the fast electron tail created by LH waves. TTMP communicates parallel energy to

the electrons. Note that it is important to take into account the formation of an electron tail created by EL and/or TTMP, as well as a minority ion tail[5] created by cyclotron acceleration. The wave damping length is considerably reduced by these non-linear effects. The energy stored in the fast particles may amount to a significant fraction of the total plasma energy and modify the plasma stability. Fast ions created by ICRF can stabilize the sawtooth instability[6] giving rise to the "monster" sawtooth regime. Current drive results from the wave-particle interaction when the suitable travelling waves are generated by the launcher. Current drive by parallel acceleration of the electrons is more efficient than minority current drive[7,8] which suffers from the generation of trapped ions. However, this latter method could be most useful for local changes of the plasma current to provide a seed current and/or to influence the plasma stability (m = 1 or m = 2 modes).

III.EXPERIMENTAL ASPECTS

The ICRH system[9] is composed of 8 identical modules (Table I) capable of delivering a total power of 32 MW. The maximum power coupled to the plasma was 22 MW. The 2 amplifiers of each generator module feeds the 2 inputs. The design was optimized to eliminate impurity release from sputtering (including self-sputtering of the screen material) by ions accelerated in the electric field produced by RF field rectification in the sheath[10,11]. Three key features characterize the design[2]:

1) The antenna is made of **low Z materials**:
   Carbon is used in the side protections and the Faraday screen is made of Beryllium bars. The self-sputtering of Beryllium and carbon being less than 1, impurity avalanche is avoided.
2) The screen bars are **tilted by 15°** in order to be approximately aligned with the local magnetic field at the antenna location. This arrangement corresponds to the wave polarisation of the fast wave and reduces the $E_{//}$ component involved in the RF sheath rectification process.

3) The 2 poloidal current straps inside the antenna box can be **phased** at arbitrary angle while keeping the strap currents constant as described later in V.A. Dipole phasing (0, π), on JET antenna, cancels the net value of $V_{//} = \int E_{//}\, dl$ taken along a line of force touching 2 antenna sides, thus eliminating the RF flux driving the RF sheath rectification process.

Features 1 and 2 alone are sufficient to reduce ICRF specific impurity generation to negligible level; however, if feature 3 is not used, we have calculated that edge convective cells[12] can be driven by the remaining $V_{//}$ component due to imperfect alignment of the screen bars with the magnetic field. The convective cell may influence the quality of the H-mode. Recent experiments show that H-modes with dipole phasing have higher confinement than when monopole (0,0) is used.

The prototype stage of the LHCD system[13] was recently brought into operation. It represents 1/3 of the final system which will be installed during the next JET shutdown. The present system is fed by 8 klystrons (3.7 GHz) rated at 600 kW. The power is then split into 128 single mode waveguides (72 x 9.5 mm^2 each). The power is split in the toroidal direction into 16 waveguides with careful control of the phase so that the antenna launches a beam with a well defined parallel spectrum typically $n_{//} = 1.8 \pm 0.2$. The system is still in a conditioning phase and the power was limited by arcing or cross talk among the waveguides to a maximum total power of 2.4 MW corresponding to a power coupling capability of 25 MW m^{-2} (we exclude here the surface of the side protection). For comparison, the ICRF coupling capability is 5 MW/m^{-2} if one refers to the screen surface facing the plasma or 42 MW m^{-2} if one refers to the surface of the 2 coaxial penetrations through the vacuum vessel. The launcher can be moved during the shot using hydraulic actuators so that the reflected power can be kept below 10 % of the incident power.

The main technical aspects of the LHCD and ICRH systems are summarized in Table I.

IV.HEATING RESULTS IN HIGH FUSION YIELD SCENARIOS

ICRH can be operated in different plasma confinement modes. The performance in terms of global energy confinement is summarized in Fig.1 which compares the "thermal" energy confinement to the DIII-D/JET H-mode scaling which has been derived from a regression analysis of H-mode data from various large tokamaks using mainly neutral beam injection. In producing the data of Fig.1, care has been taken to remove from the stored energy measurements the energy contained in the fast minority ions driven by ICRH ($W_{fast} < 0.15$ W_{kin} for the data of Fig.1). We have used the definition:

$$\tau^{H}_{FIT} = 0.106\ P^{-0.46}\ I_p^{1.03}\ R^{1.48} \qquad \text{(DIII-D/JET H-mode scaling)}$$

and

$$\tau_{Norm} = \tau_{thermal}/\tau^{H}_{FIT};\ \tau_{thermal} = \frac{W_{kin}}{P_{loss}}$$

In the following sections, we describe the aspects specific to ICRF in each mode.

A <u>L-mode Regime: D-He^3 Fusion Experiments. High Minority Concentration Regime</u>

The global confinement is found to be $\tau_{norm} \simeq 0.65$ for power scans up to 23 MW. In these experiments, the plasma current was 3 MA, $B_\phi = 2.8$ T and the plasma was resting on the belt limiters made of Beryllium tiles. The volume averaged electron density was in the range of 2 to 5 10^{19} m^{-3}. Z_{eff} was between 1.5 and 2.5 (Deuterium plasma, H minority) and $P_{rad}/P_{tot} \sim 0.1$ to 0.3. This value of τ_{norm} is somewhat larger than standard L-mode confinement presumably because of the narrow central power deposition. The sawtooth duration in this regime was larger or comparable to the energy confinement time.

At moderate plasma density ($\sim 2.5\ 10^{19}$ m^{-3}) very long sawtooth-free discharges (up to 7 seconds) are obtained using stabilisation by fast minority ions. Central electron temperatures in

the range of 10 to 13 keV could be reached (see Figs 9 and 12 of ref 2) which are suitable to D-^{3}He fusion experiments. The ICRH frequency was adjusted to the ^{3}He ion cyclotron resonance near the magnetic axis and the concentration of the minority ^{3}He ions was controlled either by gas puffing and/or using central ^{3}He deposition by the NBI system. The concentration $n_{^3He}/n_e$ was varied between 0.03 and 0.15. With 14 MW of ICRH power, the ^{3}He-D fusion power reached 140 kW (4.6 10^{16} reaction/s) corresponding to fusion multiplication factor $Q \simeq$ 1.25 %. The fusion power increased with the energy stored in the fast ^{3}He ions (Fig.2) in agreement with a theoretical model[14] which describes the non-maxwellian distribution function of the ^{3}He ions driven by ICRH. The results are consistent with the development of a high energy tail with a perpendicular temperature of 1 MeV which corresponds to the optimum of the D-^{3}He cross section. These fusion experiments are a benchmark of a (D)-T ignition scenario where the species at cyclotron resonance would be deuterium instead of ^{3}He and tritium would take the role of the majority species played by deuterium in the present experiments.

The (D)-T scenario is required to work at higher density (~ 10^{20} m^{-3}) and at higher minority concentration $n_d/n_e \sim 0.2$ to 0.3 in order to prevent the high energy tail of the deuterons to exceed the optimum value corresponding to the largest D-T cross section. The possibility of working at high concentration has recently been demonstrated[15]. It implies the use of a radiated spectrum rich in components at high $k_{//}$ values ($k_{//} \sim 7$ m^{-1}) in order to avoid the onset of the mode conversion layer associated with the 2 species hybrid resonance[16,17].

B H-mode Regime

Long duration H-modes could readily be obtained as soon as dipole phasing and beryllium evaporation were used in standard JET 3 MA double null plasmas[18]. The use of beryllium screens made beryllium evaporation redundant. Further progress in operational flexibility was made after the installation of a feedback loop acting on the radial plasma position to maintain the real part of the antenna loading resistance constant during the H-mode transition (Fig 3). At the same time, a frequency feedback loop is used to compensate for the variation of the imaginary part of the loading resistance. The distance between the separatrix and the

antenna protection needs to be more than 2 cm to obtain an H-mode but once the H-mode is formed this distance is reduced to 1 cm by the feedback system without deleterious effect on the H-mode. With dipole phasing in 3 MA plasmas τ_{norm} ranges between 1 and 1.4. In this condition, the H-mode is elm-free with long sawtooth-free period (~ 1 second). The termination of the elm-free period is caused by a carbon bloom when more than 15 MJ have been conducted to the x-point tiles. Longer H-mode (~ 3 seconds) can be obtained by modification[19] to the plasma edge either by gas puffing in the x-point region or using nickel impurity injection by the laser blow-off technique or by moving the separatrix close to the antenna. Elms or low amplitude grassy elms are developed by this method resulting in a larger average scrape-off layer and lowering by a factor 3 to 5 the particle confinement time with a modest reduction of τ_{norm} by about 20 %. A similar behaviour has been observed in NBI only H-mode or in combined NBI/ICRH heating. An example of a 7 second long elmy H-mode is given in Fig 4. Elms appear when the discharge is moved towards the ICRF antennae. The distance between the antenna side protections and the separatrix is $d \leq 0.01$ m producing enhanced recycling near the antenna protections. Incidentally, the heating scenario in this case was the third harmonic of deuterium and the wave was mainly damped on the deuterium beam ions increasing plasma fusion reactions.

C PEP, PEP + H, Hot Ion H-modes

Regimes with improved central confinement are produced either with deep pellet injection "PEP (PEP for Pellet Enhanced Phase) or by strong fuelling of a low target density plasma with Neutral Beam Injection (hot ion mode). It is possible to combine the improved central confinement regime with the improvements resulting from the H-mode. We call these high performance regimes "PEP + H"[20] and "hot ion H-modes". They correspond to a triple product $n_d \tau_E T_{io} \sim 7.8\ 10^{20}$ m^{-3} s keV for the PEP + H or $9.5\ 10^{20}$ for the hot ion H-mode[21]. τ_{norm} reaches 1.6 and 1.5 respectively. However, the optimism generated by these results should be moderated by the fact that the duration of the high confinement phase could not be extended beyond 1.5 seconds either due to a carbon bloom or due to MHD instabilities.

ICRH was the main heating method used in the discovery of the PEP and PEP + H regimes in JET because of its ability to re-heat a densified core ($n_{eo} \sim 1.2\ 10^{20}\ m^{-3}$) with a power deposition profile peaked on axis. More recently, it has been possible to increase the central ion temperature obtained in the PEP by using 2 frequencies (48 MHz and 36 MHz) accelerating 2 different minorities: hydrogen and helium 3. This method reduces the minority tail temperature driven by ICRH, so that the power heating directly the ions is increased to about 60 % of the input power. Peak ion temperatures ranging from 16 to 18 keV and peak electron temperature from 12 to 14 keV have been obtained with this method (Fig 5).

In the hot ion H-mode, ICRH has been limited to low power levels ($P_{ICRF} < 0.2\ P_{NBI}$) because the total power on the x-point target plates is limited by the carbon bloom phenomenon. Replacing 15 % of the NBI power by RF will maintain constant the total D-D reaction rate by increasing the peak electron temperature by about 10 %. Despite a very limited number of attempts (6 shots), high performance discharges have been obtained (Table II)

D High Bootstrap Current and High τ_{norm} with ICRH

Large values of $\tau_{norm} \simeq 1.7$ to 1.8 (eg 3.6 $\tau_{Goldston}$) have been observed with ICRF heating at low plasma current in double null x-point plasmas. After an elmy period which lasts 1.1 seconds, the discharge evolves into an elm-free phase (Fig 6) where the D-D reaction rate, the density and the kinetic energy nearly triples while the energy contained in the fast particles which was initially a significant part of the total energy content decreases to a negligible value. The sawteeth disappear early in the elm-free phase. The central pressure corresponds to $\beta_p \simeq 2$. The surface loop voltage is negative during the H-mode phase. Such a behaviour is well simulated (Fig 7a), by a time-dependent current diffusion code[22] incorporating neo-classical bootstrap current as a source term. The agreement between the simulation and the experiment implies that about 70 % of the current is driven non-inductively[23,24] with a broad profile in general agreement with neo-classical bootstrap terms. The broad bootstrap current is responsible for the decrease of the inductance. It is interesting to note that the confinement improves gradually while l_i decreases, at least by $\approx$ 30 %, in sharp contrast with L-mode ramp-up and ramp-down experiments.

The improved confinement terminates abruptly after 2 seconds (Fig 6). At this stage of the analysis it is not clear whether the termination is due to MHD instability.

V. CURRENT DRIVE RESULTS

A Minority Fast Wave Current Drive

Fish first noted[7] that minority ion cyclotron heating, despite the fact that it gives perpendicular energy can produce current drive with fast waves travelling preferentially in the toroidal direction due to the change of collisionality of the resonating ions. The resonant condition $\omega - \omega_{ci} = k_{//} V_{//i}$ implies that the sign of the driven current reverses on the 2 sides of the resonance layer leading to a small net current when, as in JET, the power damped on the 2 sides of the resonance are similar (note that in reactor grade plasmas the damping will be nearly one-sided). However, the effect can modify the local gradient of the plasma current density which in turn can have a strong effect on the stability of internal modes.

The minority current drive experiment was performed with ±90° phasing between the current of the 2 straps within an antenna housing. A new control system[25] provides automatic impedance matching while maintaining constant the antenna current and phase difference. Such a procedure is necessary in order to launch a well defined spectrum of travelling waves (Fig.8). It implies an imbalance in the forward power driving the 2 antenna straps. The wave directivity $\delta = \frac{P_+ - P_-}{P_+ + P_-}$ was $\simeq$ 0.3 - 0.6 with 90°. Finally the wave frequency was chosen so that the Hydrogen cyclotron resonance was moved around the q = 1 surface on the high field side of the torus so that local current drive effects would modify the stability of the sawtooth instability.

The results of the experiments which are summarized in Fig 9 clearly show a strong effect on the sawtooth instability. The effect on the sawtooth activity is either destabilizing ($\tau_{st} \simeq 0.04$ sec) with -90o phasing or stabilizing ($\tau_{st} \sim 1$ sec) with the reverse phase. The effect is maximum for power 4 MW (Fig 9). The cyclotron resonance was at R = 2.72 ± 0.05 m and the inversion radius at R = 2.80 ± 0.05 m. No effect is observed when the resonance is on-

axis. Placing the resonance at the q = 1 location on the low field side produces a weaker effect and the sign of the phase for stabilisation needs to be inverted.

These observations are in qualitative agreement with expectations derived from minority fast wave current drive effects. Stabilisation results from the decrease in the shear of the poloidal field[6] near the q = 1 surface. Calculations[8] show that minority current drive produces the required change of current profile. The optimum power level and the reduction of efficiency at higher power is expected as the protons gain perpendicular energy; firstly they tend to become trapped and secondly they slow down mainly on electrons for $E > E_{crit}$. In this case the relative drift between the 2 ion species is lost. Finally, 2 physics aspects are calculated to be modified when the experiment is performed on the low field side: firstly the number of trapped minority ions increase considerably thus reducing the current drive efficiency, secondly the sign of the phase requested to produce a given change of shear is reversed. Detailed analysis of the processes are in progress.

Minority current drive and neutral beam current drive obey the same scaling[7]: $I/P(A/W) \simeq 2\ 10^2\ (T_{eo}/R_1\ n_{14})\ (J/P_d)$ where J/Pd is dimensionless and depends on the current drive mechanism. The efficiency is therefore expected to rise considerably with the electron temperature. Thus the minority current drive has considerable potential for controlling the current profile in the center without density restrictions which affects all other methods. Finally we point out that sawtooth control is a very fast method to control the fusion burn in a tokamak.

B <u>Current Drive with Slow Waves and Synergism with the Fast Wave: Long Pulse Operation</u>

A considerable data base has been assembled on the physics of Lower Hybrid current drive and on its performance on tokamaks[26]. The current drive efficiency is generally measured by $\gamma = I_{CD} < n_e > R/P_d$ where I_D refers to the non-inductive current driven by the injected power P_D. γ is seen in the JT-60 tokamak[27] to increase with the peakedness of the radiated spectrum and with the plasma electron temperature up to $\gamma \simeq 0.34\ 10^{20}\ m^{-2}\ A/W$..

The first experiments in JET[2,13] were aimed at the determination of the fast electrons created by LH waves taking advantage of the large dimensions of the JET plasma and using a camera detecting the Bremstrahlung radiation emitted by the fast electrons[28]. The spatial distribution of the fast electrons was found to depend on the plasma density and on the magnetic field in general agreement with accessibility conditions of the slow wave. Fast electrons profiles are peaked on-axis when $n_{eo} \leq 2.4\ 10^{19}\ m^{-3}$ and $B_\phi = 3.4$ T.

Figures 10a, b and 11 summarize the information obtained with the fast electron camera when the density is close to the accessible density. The hollowness of the distribution increases with energy and density[29], an observation also made on Tore Supra[30]. The distribution of high energy photons (Fig 11) exhibits a tail characterized by a slope T_{photon} which increases with LH power. T_{photon} can increase further up to $T_{photon} \simeq 150$ keV when the plasma is heated by fast waves. This synergistic effect has been seen when the density is below the critical density and when monopole phasing is used (H minority, 48 MHz). Experiments performed with dipole phasing did not reveal any increase of T_{photon} beyond the value obtained with LH alone. It is a significant feature of this experiment that electrons are accelerated beyond the highest energy corresponding to the $n_{//}$ spectrum of the launched LH waves ($\simeq$ 100 keV) even when the loop voltage is zero. A plausible explanation of this phenomenon has been proposed recently[31] to be the result of direct electron damping of the fast wave (mainly by TTMP) on the fast electron created by LHCD. About 10 % of the ICRH power is damped in this way when a 1 % electron population is assumed to have a 200 keV isotropic temperature. This process diverts power which would normally have been damped by minority heating. The additional acceleration of the fast electrons reinforces the unidirectional nature of the population and contributes to the current drive[32]. We will include this effect in the term P_d when the efficiency γ is determined.

This synergistic mode of operation corresponds to the highest current drive efficiency observed on JET. A plasma current of 1.5 MA has been sustained with zero loop voltage for 3 seconds at a central density of $2.4\ 10^{19}\ m^{-3}$ (Fig 12) . This current is produced by 2.1 MW of LH power supplemented by an estimated ~ 0.6 to 1 MW from the fast wave. 1 MW contribution to P_d from the total ICRH power in excess of 5 MW is an upper estimate and in

that sense the derived efficiency $\gamma = 0.4$ is the lower estimate. The range of P_d was obtained by modulating the LHCD power (with and without ICRH). The error bar of the estimate is denoted in Fig 13.

The current drive efficiency, γ is represented in Fig 13 for a number of current drive situations. In determining γ, care has been taken to substract from I_{CD} the bootstrap contribution (using the neoclassical formula) and to include in P_d both the contributions from the fast wave and from the loop voltage[32]. For comparison with JT-60, the data is plotted as a function of $< T_e >$ although the influence of the T_e increase and of the synergism are mixed since both effects come from ICRH. In order to clarify the importance of the various contributions to γ, first consider, in Fig 3, the results without synergism (LH only, LH + ICRF (dipole)); γ increases with $< T_e >$ but the highest value is only $0.2\ 10^{20}$. Adding synergism at fixed T_e value brings γ up to $0.3\ 10^{20}$. This result can be understood by noting that the higher energy electron experiences a smaller drag and is therefore more efficient at driving current. Increasing simultaneously $< T_e >$ and the synergistic contribution (squares and triangles) brings γ up to $0.4\ 10^{20}$. It is conceivable that γ can be increased even further by optimizing the amount of fast wave power going to the fast electrons.

Contrary to the bootstrap current drive experiments, the current drive with LH and fast wave has a similar spatial distribution as the ohmic current drive: $l_i \simeq 1.4$ to 1.8 and changes by about 10 % during the current drive phase. Consequently full current drive experiments such as in Fig 12 are close to steady state. As a final remark we stress that both RF systems have been used to extend the JET pulse length to one minute[29]. Fig 14 shows that the one minute plasma has an electron temperature of 4 keV. The plasma pollution remains low during the entire pulse ($Z_{eff} \simeq 1.75$) and D-D fusion reaction rate remains constant. The total energy delivered to the plasma reached 280 MJ.

VI.CONSEQUENCES FOR FUTURE DEVICES AND CONCLUSIONS

After reviewing the recent JET experiments, it is appropriate to discuss their significance in the light of applications which have been proposed[33] for International Thermonuclear Experimental Reactor (ITER). Such applications are summarized in Table III. The proposed

ICRH system is wide band as in JET covering the frequency range between 17 and 66 MHz. In each module of 2 to 3 MW, it is possible to set within this range a frequency appropriate to a specific application and to change it during the pulse. The proposed LHCD system is in the range of 6 GHz which is appropriate for current drive in the outer plasma half. The most efficient current drive scenario with waves avoids all cyclotron damping; it corresponds to the 17 MHz and 6 GHz mixture (scenario 1 of Table III). The recent current drive result reported in chapter V.B are relevant to scenario 1; we should however stress that our results have been obtained with a density of 2.4 10^{19} m^{-3} and should be extended to experiments at higher density. Note that in the present experiment, the damping per pass via TTMP is quite low making the experiments difficult. Working at high β_e on JET should improve the situation. Scenarios 2, 3, 5 of Table III are all based on central cyclotron damping. There is a worldwide data base substantiating the claim that this heating mode is most attractive for ITER. The specific contributions of JET to these scenarios are: for scenario 2, the demonstration of central ion heating with high minority concentration and the high density operation with the PEP; for scenarios 2 and 3, the first demonstration of minority current drive with fast waves leading to active control of the sawteeth via current profile control near the q = 1 resonance region. JET made also good progress in the field of advanced fuel reactors by demonstrating 140 kW of D-^{3}He fusion power for several seconds. This experiment was designed as a bench mark of the D/T ignition scenario.

In conclusion, the results presented in this article considerably strengthen the case for heating high density reactor plasmas with waves and show the versatility of use in many different regimes. Antenna design has reached a mature state where RF specific impurity production is never a problem. Experiments on current drive have only just started. Three current drive modes have been explored: LHCD alone, LHCD and fast wave synergism and minority fast wave current drive. The results obtained with LHCD alone are consistent with previous observations, the synergism and minority current drive are very new observations. The JET data strongly support the interpretation that the fast wave further accelerates the fast electrons driven by LHCD. However the data base is still sparse. The γ value 0.4 10^{20} is somewhat higher than the best value 0.34 10^{20} previously obtained on JT-60. It still needs to

be further improved if full current drive in steady sate reactors is to become an economical option and there is a need for more experimentation of these regimes.

The next stage of the JET LHCD system will be a 3-fold increase in power launching capabilities (Table I); in addition new ICRH antennas are being constructed in order to match the JET pumped divertor geometry. The 4 strap antenna design will allow a sharper and more directive fast wave spectrum to be generated. These new equipments will be used to enlarge the data base for the ITER heating and current drive scenarios and may also reveal new regimes.

REFERENCES

[1]Rebut, P-H., Watkins, M. L., Gambier, D. J., and Boucher, D., Phys. Fluids B3(8), 2209(1991).

[2]Jacquinot, J. and the JET Team, Plasma Phys. and Contr. Fus. 33, (1991)1657.

[3]Goldston, R., Plasma Phys. and Contr. Fus. Vol.26 (1984)87.

[4]Start D. F. H., Bartlett, D. V., Bhatnagar, V. P., Campbell, D. J., Challis, C. D., Corti, S., Cheetham, A., Edwards, A. W., Eriksson, L-G., Gill, R. D., Gottardi, N., Hellsten, T., Jacquinot, J., Mayberry, M. J., Rimini, F. G., Salmon, N. A., Smeulders, P. and Von Hellermann M., Nucl. Fus. 30 (1990)2169.

[5]Stix, T. H., Nucl. Fus. 15 (1975)737.

[6]Porcelli, F., Plasma Phys. and Contr. Fus. 33, 1601(1991).

[7]Fish, N., J., Nucl. Fus. 21 (1981)15

[8]Start, D. F. H., Bhatnagar, V. P., Bosia, G., Brusati, M., Bures, M., Campbell, D. J., Challis, C. D., Cottrell, G. A., Cox, M., Edwards, A., Eriksson, L-G., Froissard, P., Gormezano, C., Gowers, C., Hugonnard, S., Jacquinot, J., Kupschus, P., Gottardi, N., O'Brien, M. R., Pasini, D., Porcelli, F., Righi, E., Rimini, F. G., Sadler, G., Tibone, F., Tubbing, B.and Von Hellermann, M. To be published in Proc. IAEA Tech. Com. Meeting on Fast Wave Current Drive in Reactor Scale Tokamaks, Arles 1991, by CEA Association Euratom-CEA , Centre d'Etudes Cadarache, edited by D. Moreau.

[9]Wade, T. J., Jacquinot, J., Bosia, G., Sibley, A., Schmid, M. S., Proc. 14th IEEE/NPSS Symp. on Fus. Eng., San Diego October 1991, published by IEEE.

[10]Bures, M., Jacquinot, J., Lawson, R., Stamp, M., Summers, H. P., D'Ippolito, D. A., and Myra, J. Plasma Phys. and Contr. Fus., Vol.33, (1991)937.

[11]D'Ippolito, D. A., Myra, J., Bures, M. and Jacquinot, J., Plasma Phys. and Contr. Fus., Vol.33, (1991)607.

[12]D'Ippolito, D. A., Myra, J., Jacquinot, J. and Bures, M., Bull. Am. Phys. Soc. II, Vol.36, (1991), p. 2341.

[13]Gormezano, C., Bosia, G., Brusati, M., Dobbing, J. A., Ekedahl, A., Froissard, P., Jacquinot, J., Kaye, A. S., Lennholm, M., Naito, O., Pain, M. S., Paoletti, F., Pasini, D.,

Ramos de Andrade, M. C., Rey, G., Rimini, F. G., Schild, P., Proc. 18th EPS Conf. Berlin 1991, (Eur. Phys. Soc., Petit-Lancy, Switzerland 1991), Vol.15C, Part III, p.393.

[14]Jacquinot, J. and Sadler G., accepted for publication in Fus. Energy and Design.

[15]Bhatnagar, V. P., Jacquinot, J., Gormezano, C., Start, D. F. H., and the JET Team. To be published in Proc. 10th Topical Conference, Charleston 1991, AIP, New York, 1992.

[16]Chrien, R. E. and Strachan, J. D., Phys. Fluids 26(7)1953.

[17]Jacquinot, J. G. and Lapierre, Y., Proc. 2nd Joint Grenoble-Varenne Inst. Symp. Conf. Vol.1, P.541(1980).

[18]Tubbing, B., Jacquinot, J., Stork, D., Tanga, A., Nucl. Fus. 29 (1989)1953.

[19]Bures, M., Campbell, D. J., Gottardi, N., Jacquinot, J., Mattioli, M., Morgan, P., Pasini, D. and Start, D. F. H., accepted for publication in Nucl. Fus.

[20]Tubbing, B., Balet, B. Bartlett, D., Challis, C. D., Corti, S., Gill, R., Gormezano, C. Gowers, C., Von Hellermann, M. Hugon, M., Jacquinot, J., Jaekel, H., Kupschus, P., Lawson, K., Morsi, H., O'Rourke, J., Pasini, D. Rimini, F. G., Sadler, G., Schmidt, G., Start, D. F. H., Stubberfield, P., Tanga, A. Tibone, F., Nucl. Fus., Vol.31, (1991),839.

[21]Keilhacker, M., and the JET Team, Plasma Phys. and Contr. Fus., Vol.33, (1991)1453.

[22]Challis, C. D., Private communication.

[23]Zarnstoff, M. C., Bell, M., G., Bitter, M., Goldston, R., Grek, B., Hawryluk, R. J., Hill, K., Johnson, D., McCune, D., Park, H., Ramsey, A., Taylor, G. and Wieland, R. Phys. Rev. Lett. Vol.60, No 13, (1988)1306.

[24]Challis, C. D., Cordey, J. G., Hamnen, H., Stubberfield, P. M., Christiansen, J-P., Lazzaro, E., Muir, D. G., Stork, D., Thompson, E., Nucl. Fus. Vol.29, No. 4 (1989)563.

[25]Bosia, G., Jacquinot, J.,.To be published in Proc. IAEA Tech. Com. Meeting on Fast Wave Current Drive in Reactor Scale Tokamaks, Arles 1991, by CEA Association Euratom-CEA , Centre d'Etudes Cadarache, edited by D. Moreau.

[26]Gormezano, C., Fus. Eng. and Des. 14(1991)99.

[27]JT60 Team Proc. 13th Int. Conf. on Plasma Physics and Controlled Nuclear Fusion Research IAEA Vol. 1 (1990) 53.

[28]Froissard, P., Brusati, M., Adams, J. M., Ekedahl, A., Gormezano, C., Jarvis, O. N., Pasini, D., Peysson, Y., Ramos de Andrade, M. C., Rimini, F. G., Sadler, G, Proc. 18th EPS Conf., Berlin 1991, (Eur. Phys. Soc., Petit-Lancy, Switzerland, 1991) Vol.15C, Part III, 389.

[29]Brusati, M., Ekedahl, Froissard, P., Gormezano, C., Jacquinot, J., Lennholm, M., Lomas, P. J., Pain, M. S., Ramos de Andrade, M. C., Rimini, F. G., Schild, P. and Start, D. F. H. To be published in Proc. 10th Topical Conference, Charleston 1991, AIP, New York, 1992.

[30]Pecquet, A-L., Hubbard, A., Moreau, D., Moret, J. M., Fall, T., Lassalle, Y., Lecoustey, P., Mattioli, M., Peysson, Y., Auge[1], N., Rodriguez, L., Talvard, M., Proc. 18th EPS Conf., Berlin 1991, (Eur. Phys. Soc., Petit-Lancy, Switzerland, 1991) Vol.15C, Part III, 349.

[31]Bhatnagar V. P., Jacquinot, J., Start, D. F. H., To be published in Proc. IAEA Tech. Com. Meeting on Fast Wave Current Drive in Reactor Scale Tokamaks, Arles 1991, by CEA Association Euratom-CEA , Centre d'Etudes Cadarache, edited by D. Moreau.

[32]Gormezano, C., Brusati, M., Ekedahl, A., Froissard, P., Jacquinot, J., Rimini, F. G., To be published in Proc. IAEA Tech. Com. Meeting on Fast Wave Current Drive in Reactor Scale Tokamaks, Arles 1991, by CEA Association Euratom-CEA , Centre d'Etudes Cadarache, edited by D. Moreau.

[33]Parail, V. V., Fujisawa, N., Hopman, H., Kimura, H., Lindquist, W.B., Nevins, W. M., Rebuffi, L., Sironi, M., Swain, D. W., Wégrowe, J-G., in ITER Documentation Fluids No 32, IAEA, Vienna, 1991 p189.

FREQUENCY	SYSTEM	POWER	LAUNCHERS	MATCHING	COUPLED POWER (MW)
LHCD 3.7 GHz slow wave	Prototype System	8 klystrons 0.6 MW each Phase control	128 waveguides in 1/3 of a main port $1.4 < n_{//} < 2.3$	• Multi-junction arrangement • Movable launcher	2.4
	Full system	24 klystrons 0.6 MW each	384 waveguides filling a main horizontal port	Can be moved during the pulse (hydraulics)	In construction
ICRH 23 to 57 MHz fast wave	"A_1" system using tilted beryllium screens and upgraded amplifiers	16 amplifiers 2 MW tetrode output each 20 seconds Phase control	8 antennae wall mounted 2 current straps in each antenna 4 strap antenna in construction (A2 system)	Feedback loops on frequency, stub, plasma position	22

Table I: Technical Specifications of the 2 JET HF Systems

Power	W_{dia}	$\frac{dw}{dt}$	R_{DD}	T_{io}	T_{eo}	n_{eo}
(MW)	(MJ)	(MW)	s^{-1}	keV	keV	m^{-3}
16 NBI + 2 RF	11.1	8.9	$8\ 10^{16}$	23.5	11.2	$2.7\ 10^{19}$

Table II: Parameters at Peak Neutron Yield during Hot Ion H-mode with Combined Heating (# 26043)

Scen-arios	ν	Resonances on axis	Damping	Function
1	17 MHz + 6 GHz	none	TTMP/E L on electrons	Current Drive Fast Wave current drive in the center LHCD off axis $\gamma = 0.3 - 0.35\ 10^{20}$
2	33 MHz	$\omega = \omega_{CD}$ on axis	• on ions if $n_D/n_T > 0.2$ • some α damping on axis	Central Ion Heating - best ignition scenario - penetration independent on density - minority current drive (profile control, burn control)
3	44 MHz	$\omega = \omega_{CHe^3}$ $\omega = 2\ \omega_{CT}$	ions/electrons	Central Heating - advanced fuel scenarios - can also be used in the non-active phase - minority current drive
4	55 MHz	none	• electron TTMP/E L • some α damping • some 2 ω_{CT}	Current Drive - higher damping per pass than in 1 but γ lower due to 2 ω_{CT} heating
5	66 MHz	$\omega = \omega_{CH}$ $\omega = 2\ \omega_{CD}$	- Hydrogen - Deuterium - α	Central Heating - for the non active phase

Table III : Proposed Heating and Current Drive Scenarios for ITER, $B_0 = 4.3$ T

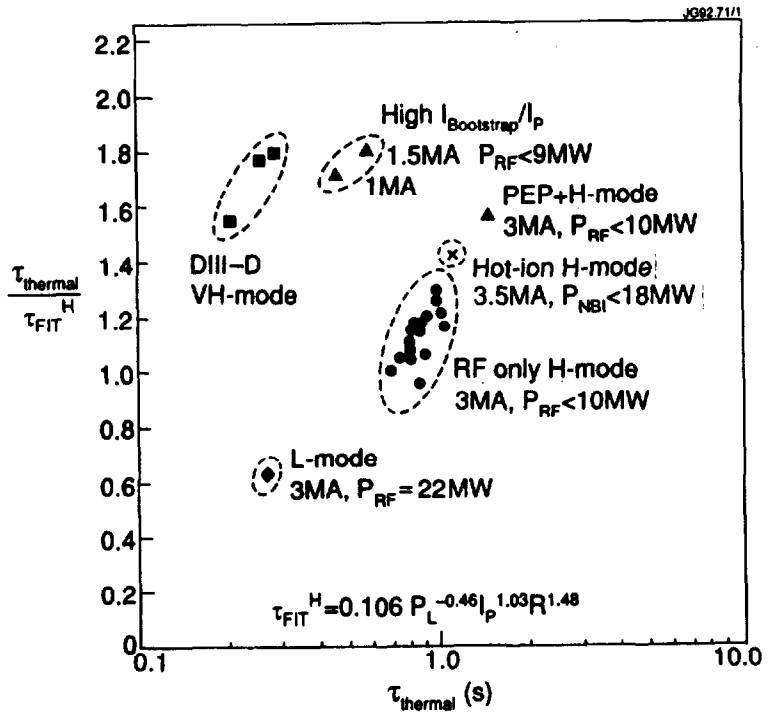

Figure 1: Normalized confinement time versus thermal confinement times for various JET confinement regimes. Also shown are DIII-D VH-mode result. $\tau_{ITER}^{H} = 0.106\ P_{loss}^{-0.46}\ I_p^{1.03} R^{1.48}$.

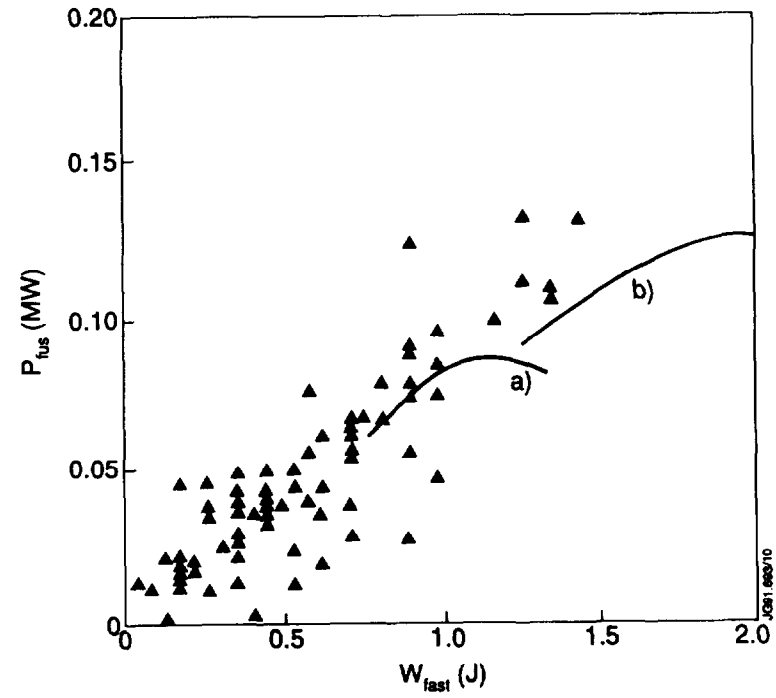

Figure 2: D-^{3}He fusion power versus the energy stored in the fast ^{3}He ions. Comparison to theoretical calculations using measured n_e and T_e with $P_{(RF\ power\ to\ 3He)}$ = 7.5 MW (a) and 10 MW (b).

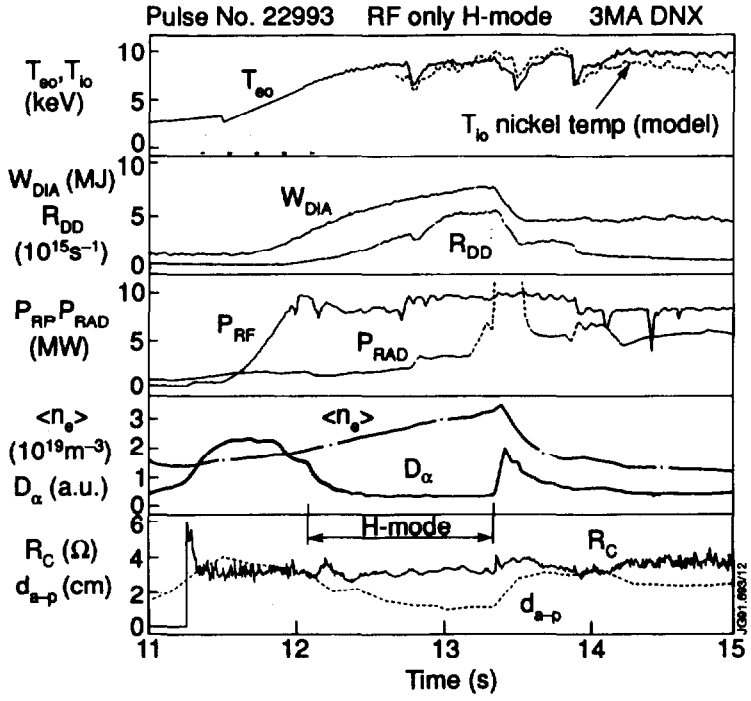

Figure 3: Experimental traces during an elm-free H-mode with dipole. Note that the loading resistance R_C is maintained constant by the feedback system. The H-mode is terminated by a carbon bloom at 13.3 seconds.

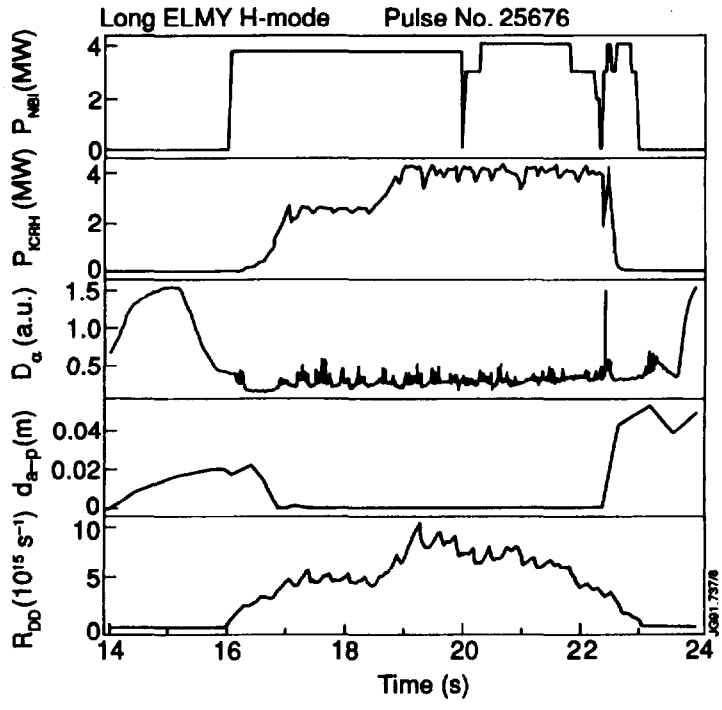

Figure 4: Standard plasma parameters of a long elmy-H-mode during combined NBI/ICRF heating. The elm behaviour is generated by moving the plasma close to the antenna. D_{ant} is the distance between the antenna side protection and the last closed surface.

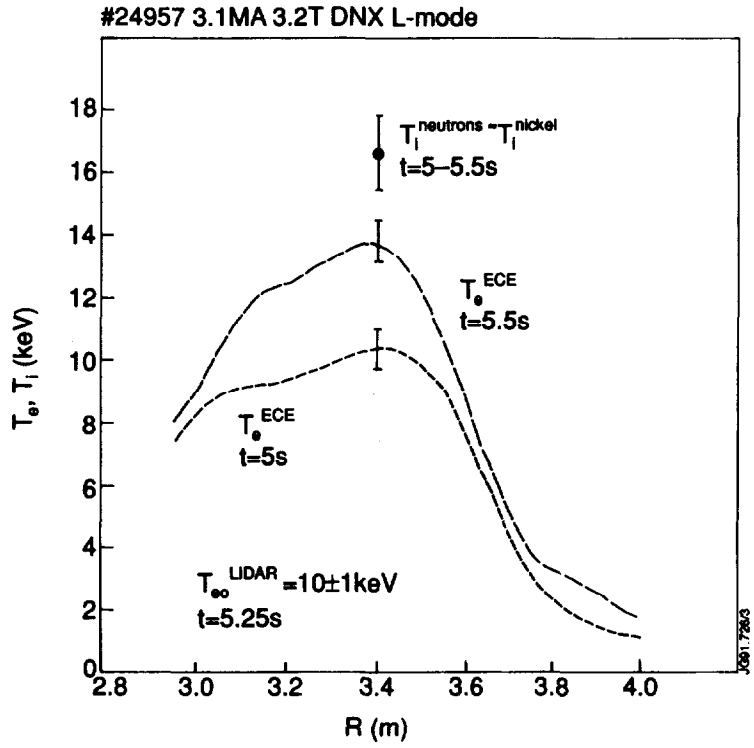

Figure 5: Electron temperature profile and central ion temperature during a PEP discharge heated with ICRH using 2 minority frequencies for H and ^{3}He.

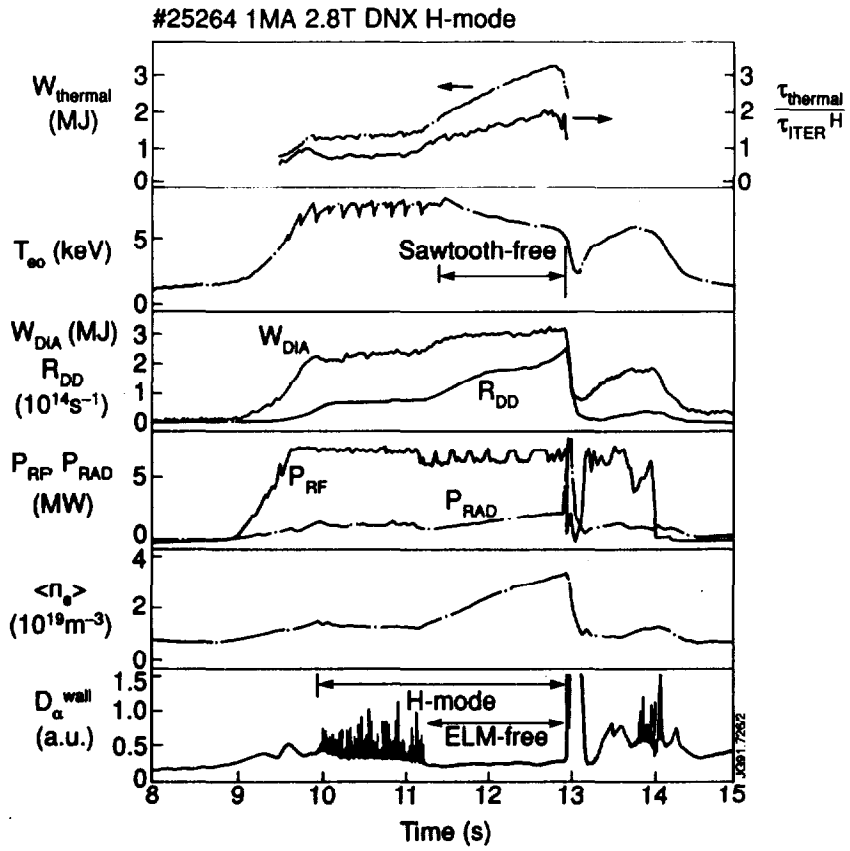

Figure 6: Evolution of plasma parameters during a 1 MA discharge giving a large bootstrap current contribution.

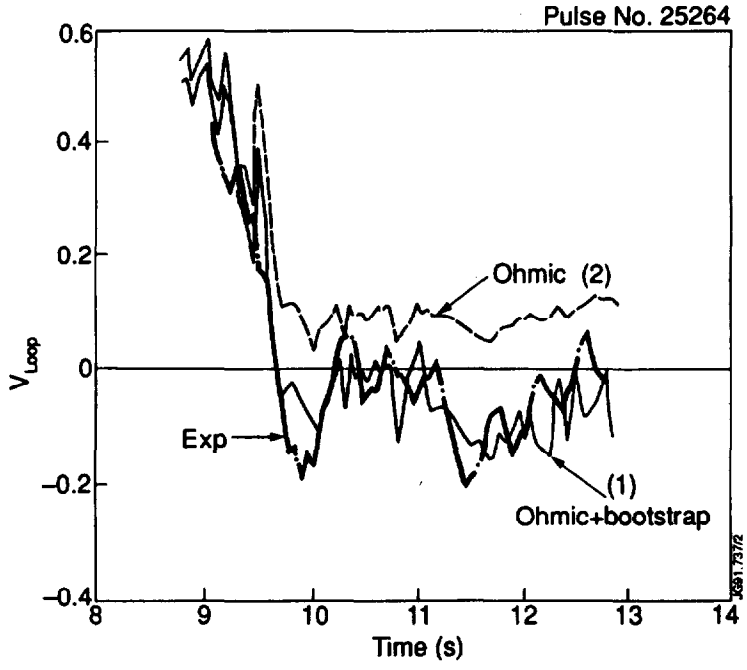

Figure 7a: Surface loop voltage versus time and comparison to a current diffusion code with (curve 1) or without (curve 2) a neo-classical bootstrap current as a source term.

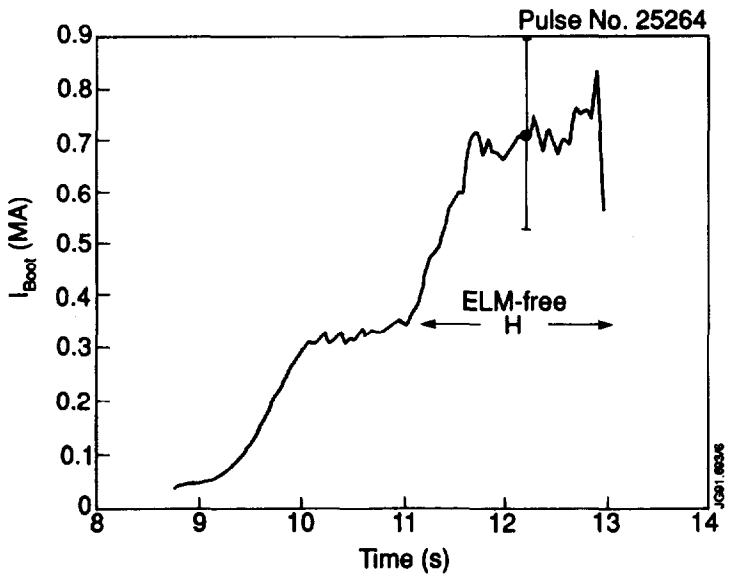

Figure 7b: Total bootstrap current deduced from the comparison of Figure 7a giving I_{boot}/I_p ~ 0.7 with an uncertainty related to the determination of the plasma equilibrium.

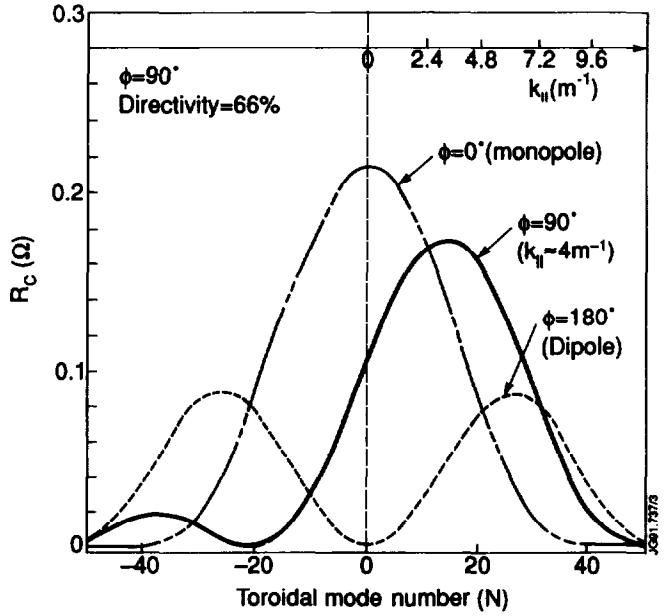

Figure 8: Spectra launched by the ICRH antenna for 3 phase differences between the 2 current straps in the antenna. The toroidal mode number is $N = k_{//}R_a$; R_a = major radius at the antenna location.

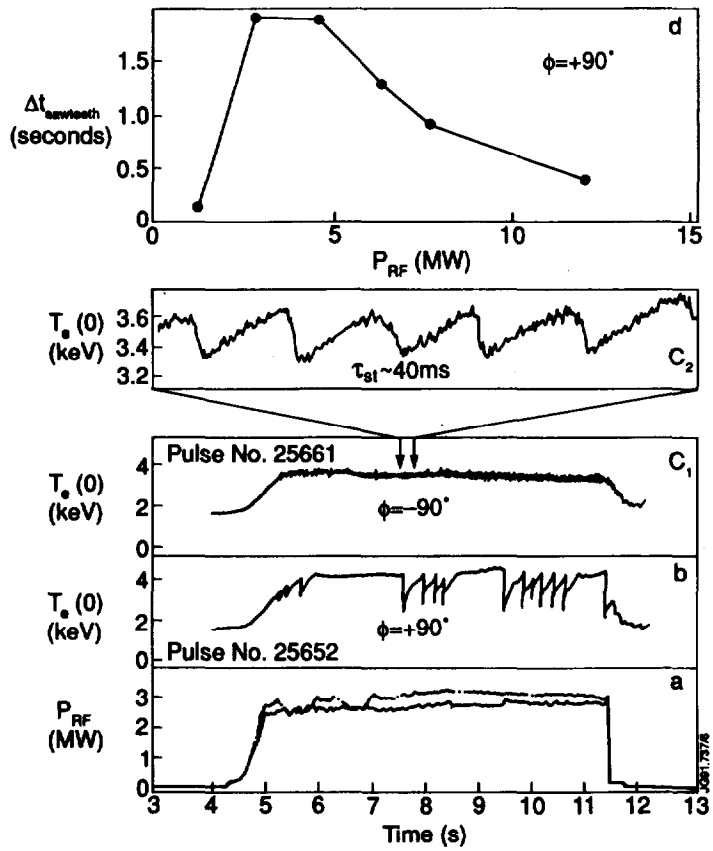

Figure 9: Minority current drive experiments with the H minority resonance tangent to the q = 1 surface on the high field side (a) RF power, (b) monster sawtooth behaviour with +90°, (C1) and (C2) sawtooth destabilisation with -90°; (d) maximum sawtooth length versus power with +90° phasing.

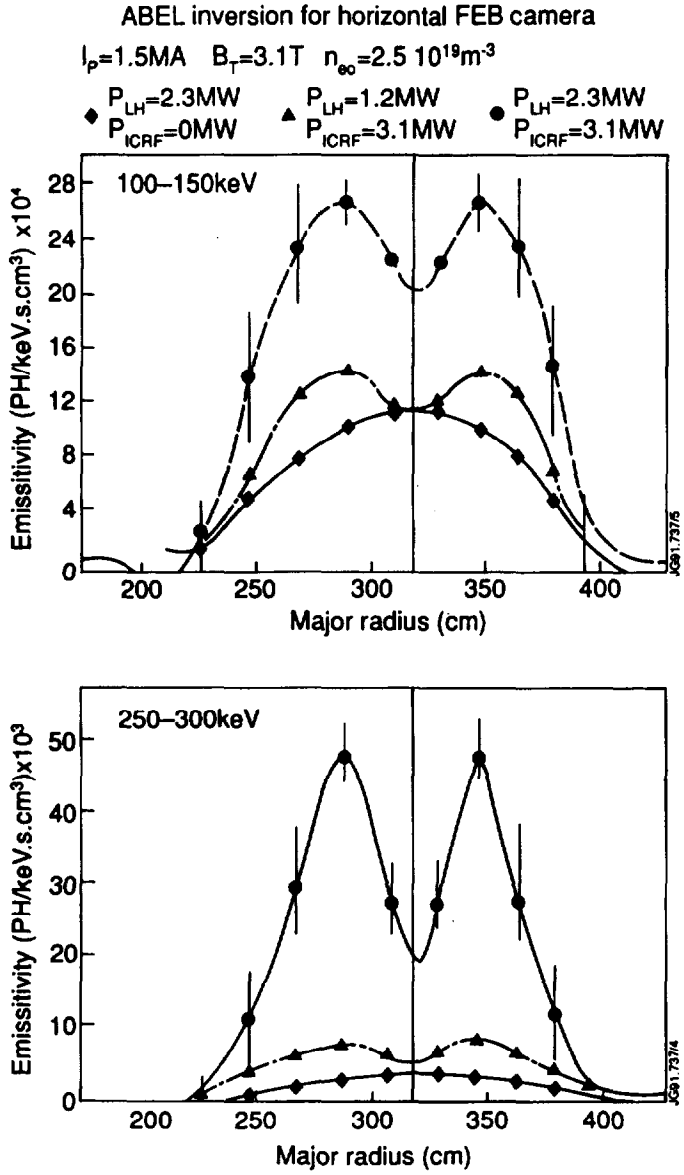

Figure 10: X-ray emissivity during LHCD experiments with and without the contribution from the fast wave (ICRH in monopole phasing) for (a) photon energy between 100 and 150 keV and (b) energy between 250 and 300 keV.

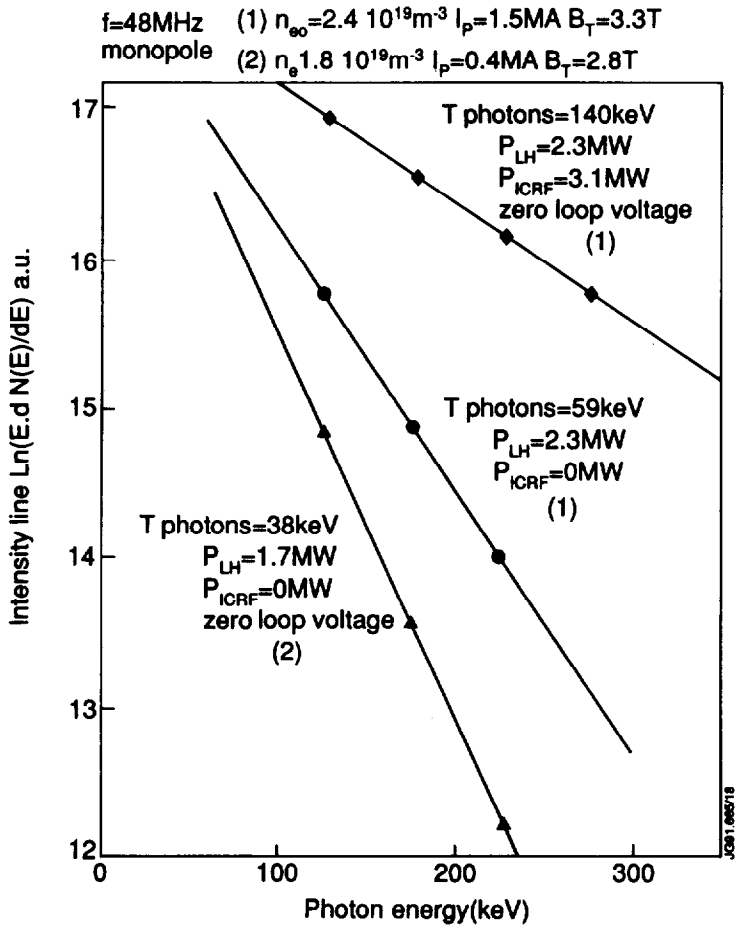

Figure 11: Spectrum of the X-ray emission during current drive experiments. The photon temperature reaches 59 keV with LH alone and 140 keV when the fast wave is added. The loop voltage drops to zero in this case.

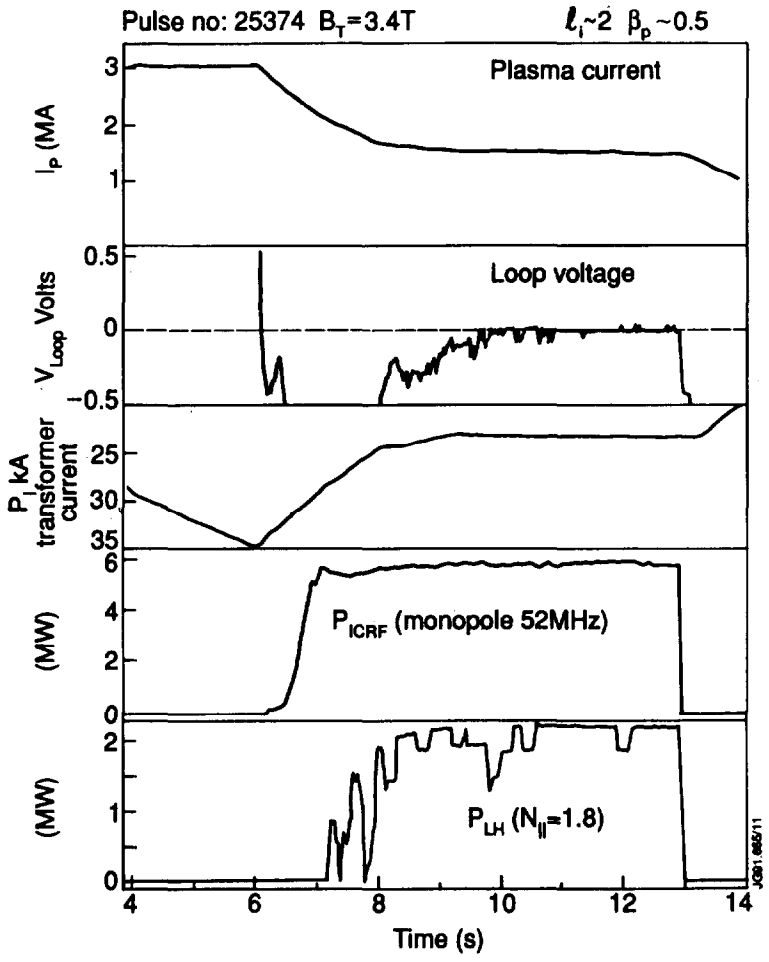

Figure 12: Plasma current, loop voltage, current in the primary circuit of the ohmic transformer, ICRH and LH powers during a current drive experiment.

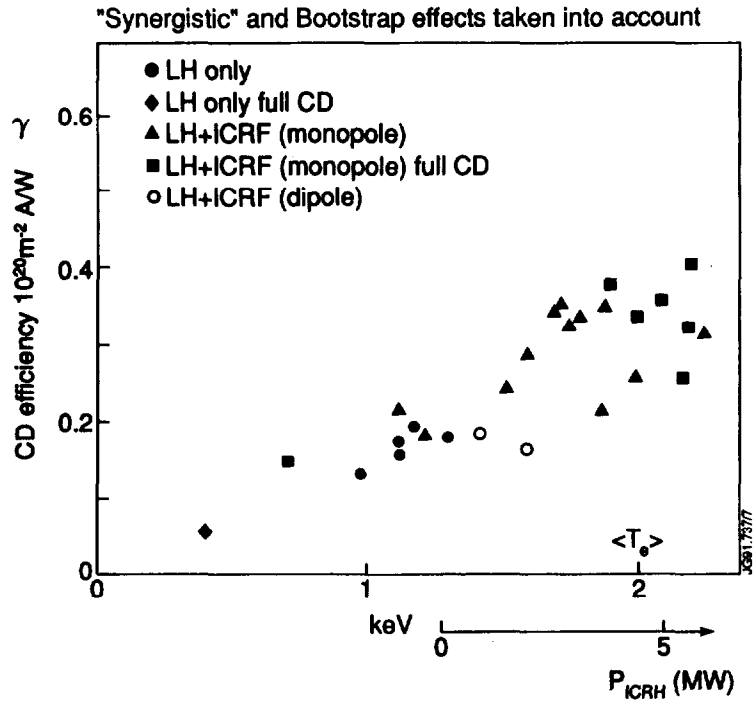

Figure 13: Current drive efficiency $\gamma = I_{CD} < n_e > R/P_d$ versus the volume average temperature for various experimental conditions. The bootstrap current is deduced from I_{CD} and P_d includes the inputs from the fast wave and from any residual loop voltage.

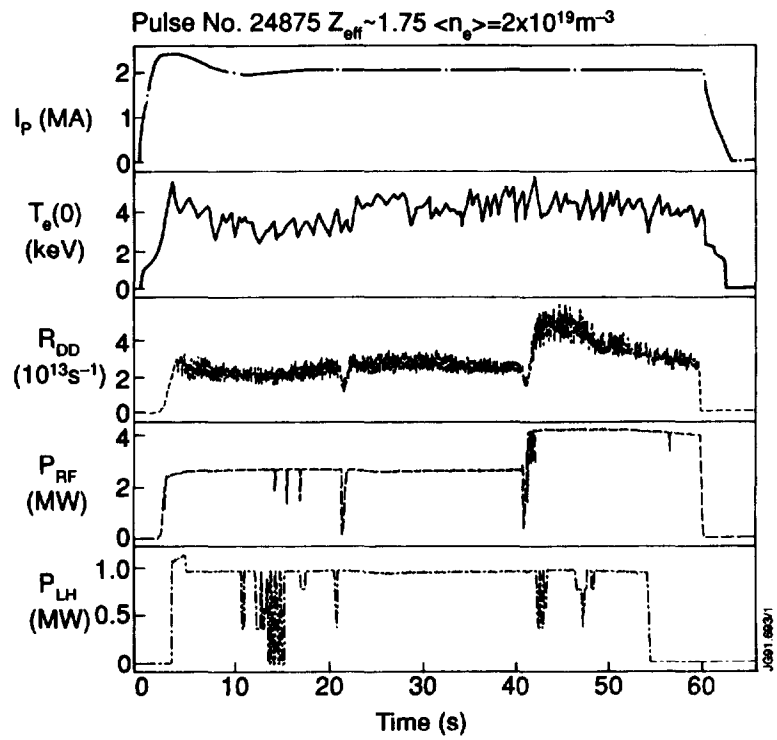

Figure 14: Plasma parameters during a one-minute pulse sustained by ICRH (180 MJ), LH (47 MJ) and ohmic power (53 MJ).

Appendix I

THE JET TEAM

JET Joint Undertaking, Abingdon, Oxon, OX14 3EA, U.K.

J.M. Adams[1], H. Altmann, A. Andersen[14], P. Andrew[18], M. Angelone[29], S.A. Arshad, W. Bailey, P. Ballantyne, B. Balet, P. Barabaschi, R. Barnsley[2], M. Baronian, D.V. Bartlett, A.C. Bell, I. Benfatto[5], G. Benali, H. Bergsaker[11], P. Bertoldi, E. Bertolini, V. Bhatnagar, A.J. Bickley, H. Bindslev[14], T. Bonicelli, S.J. Booth, G. Bosia, M. Botman, D. Boucher, P. Boucquey, P. Breger, H. Brelen, H. Brinkschulte, T. Brown, M. Brusati, T. Budd, M. Bures, T. Businaro, P. Butcher, H. Buttgereit, C. Caldwell-Nichols, D.J. Campbell, P. Card, G. Celentano, C.D. Challis, A.V.Chankin[23], D. Chiron, J. Christiansen, C. Christodoulopoulos, P. Chuilon, R. Claesen, S. Clement, E. Clipsham, J.P. Coad, M. Comiskey[4], S. Conroy, M. Cooke, S. Cooper, J.G. Cordey, W. Core, G. Corrigan, S. Corti, A.E. Costley, G. Cottrell, M. Cox[7], P. Cripwell, H. de Blank[15], H. de Esch, L. de Kock, E. Deksnis, G.B. Denne-Hinnov, G. Deschamps, K.J. Dietz, S.L. Dmitrenko, J. Dobbing, N. Dolgetta, S.E. Dorling, P.G. Doyle, D.F. Düchs, H. Duquenoy, A. Edwards, J. Ehrenberg, A. Ekedahl, T. Elevant[11], S.K. Erents[7], L.G. Eriksson, H. Fajemirokun[12], H. Falter, D. Flory, J. Freiling[15], C. Froger, P. Froissard, K. Fullard, M. Gadeberg, A. Galetsas, D. Gambier, M. Garribba, P. Gaze, R. Giannella, A. Gibson, R.D. Gill, A. Girard, A. Gondhalekar, C. Gormezano, N.A. Gottardi, C. Gowers, B.J. Green, R. Haange, G Haas, A. Haigh, G. Hammett[6], C.J. Hancock, P.J. Harbour, N.C. Hawkes[7], P. Haynes[7], J.L. Hemmerich, T. Hender[7], F.B. Herzog, R.F. Herzog, J. Hoekzema, J. How, M. Huart, L Hughes, T.P. Hughes[4], M. Hugon, M. Huguet, A. Hwang[7], B. Ingram, M. Irving, J. Jacquinot, H. Jaeckel, J.F. Jaeger, G. Janeschitz[13], S. Jankowicz[22], O.N. Jarvis, F. Jensen, E.M. Jones, L.P.D.F. Jones, T.T.C. Jones, J-F. Junger, E. Junique, A. Kaye, B.E. Keen, M. Keilhacker, G.J. Kelly, W. Kerner, R. Konig, A. Konstantellos, M. Kovanen[20], G. Kramer[15], P. Kupschus, R. Lässer, J.R. Last, B. Laundy, L. Lauro-Taroni, K. Lawson[7], M. Lennholm, A. Loarte, R. Lobel, P. Lomas, M. Loughlin, C. Lowry, B. Macklin, G. Maddison[7], G. Magyar, W. Mandl[13], V. Marchese, F. Marcus, J. Mart, E. Martin, R. Martin-Solis[8], P. Massmann, G. McCracken[7], P. Meriguet, P. Miele, S.F. Mills, P. Millward, R. Mohanti[17], P.L. Mondino, A. Montvai[3], S. Moriyama[28], P. Morgan, H. Morsi, G. Murphy, M. Mynarends, R. Myrnäs[16], C. Nardone, F. Nave[21], G. Newbert, M. Newman, P. Nielsen, P. Noll, W. Obert, D. O'Brien, J. O'Rourke, R. Ostrom, M. Ottaviani, M. Pain, F. Paoletti, S. Papastergiou, D. Pasini, A. Peacock, N. Peacock[7], D. Pearson[12], R. Pepe de Silva, G. Perinic, C. Perry, M. Pick, R. Pitts[7], J. Plancoulaine, J-P. Poffé, F. Porcelli, L. Porte[19], R. Prentice, S. Puppin, S. Putvinsko[23], G. Radford[9], T. Raimondi, M.C. Ramos de Andrade, P-H. Rebut, R. Reichle, E. Righi, F. Rimini, D. Robinson[7], A. Rolfe, R.T. Ross, L. Rossi, R. Russ, P. Rutter, H.C. Sack, G. Sadler, G. Saibene, J.L. Salanave, G. Sanazzaro, A. Santagiustina, R. Sartori, C. Sborchia, P. Schild, M. Schmid, G. Schmidt[6], B. Schunke, S.M. Scott, A. Sibley, R. Simonini, A.C.C. Sips, P. Smeulders, R. Stankiewicz[27], M. Stamp, P. Stangeby[18], D.F. Start, C.A. Steed, D. Stork, P.E. Stott, T.E. Stringer, P. Stubberfield, D. Summers, H. Summers[19], L. Svensson, J.A. Tagle[21], A. Tanga, A. Taroni, A. Tesini, P.R. Thomas, E. Thompson, K. Thomsen, J.M. Todd, P. Trevalion, B. Tubbing, F. Tibone, E. Usselmann, H. van der Beken, G. Vlases, M. von Hellermann, T. Wade, C. Walker, R. Walton[6], D. Ward, M.L. Watkins, M.J. Watson, S. Weber[10], J. Wesson, T.J. Wijnands, J. Wilks, D. Wilson, T. Winkel, R. Wolf, B. Wolle[24], D. Wong, C. Woodward, Y. Wu[25], M. Wykes, I.D. Young, L. Zannelli, Y. Zhu[26], W. Zwingmann.

PERMANENT ADDRESSES

1. UKAEA, Harwell, Didcot, Oxon, UK.
2. University of Leicester, Leicester, UK.
3. Central Research Institute for Physics, Academy of Sciences, Budapest, Hungary.
4. University of Essex, Colchester, UK.
5. ENEA-CNR, Padova, Italy.
6. Princeton Plasma Physics Laboratory, New Jersey, USA.
7. UKAEA Culham Laboratory, Abingdon, Oxon, UK.
8. Universidad Complutense de Madrid, Spain.
9. Institute of Mathematics, University of Oxford, UK.
10. Freien Universität, Berlin, F.R.G.
11. Swedish Energy Research Commission, S-10072 Stockholm, Sweden.
12. Imperial College of Science and Technology, University of London, UK.
13. Max Planck Institut für Plasmaphysik, Garching bei München, FRG.
14. Risø National Laboratory, Denmark.
15. FOM Instituut voor Plasmafysica, 3430 Be Nieuwegein, The Netherlands.
16. University of Lund, Sweden.
17. North Carolina State University, Raleigh, NC, USA
18. Institute for Aerospace Studies, University of Toronto, Downsview, Ontario, Canada.
19. University of Strathclyde, 107 Rottenrow, Glasgow, UK.
20. Nuclear Engineering Laboratory, Lapeenranta University, Finland.
21. CIEMAT, Madrid, Spain.
22. Institute for Nuclear Studies, Otwock-Swierk, Poland.
23. Kurchatov Institute of Atomic Energy, Moscow, USSR
24. University of Heidelberg, Heidelberg, FRG.
25. Institute for Mechanics, Academia Sinica, Beijing, P.R. China.
26. Southwestern University of Physics, Leshan, P.R. China.
27. RCC Cyfronet, Otwock Swierk, Poland.
28. JAERI, Naka Fusion Research Establishment, Ibaraki, Japan.
29. ENEA, Frascati, Italy.

At 1st June 1991